

Research Article

Usability of alloys with different composition as electrode for electrochemical reduction of ferricyanide ion

İlhan Altay[1] · Sinan Yapici[1] · Nizamettin Demirkiran[1]

Received: 11 February 2021 / Accepted: 23 February 2022
Published online: 01 April 2022
© The Author(s) 2022 OPEN

Abstract
An experimental work was performed to investigate the usability of 8 metallic alloys with different composition in electrochemical limiting diffusion current technique employing the cathodic reduction of ferricyanide. All the alloys exhibited a limiting current plateau region in their voltage–current behaviour, but not all gave a wide and smooth plateau, except one with almost pure Ni. With the alloys of including more than 50% Ni, as Ni ratio of the metal increased, smoother and wider plateau was attained, and the electrode containing 99% Ni gave the smoothest plateau. The other alloys tested can only be used as electrode in the limiting diffusion current technique in low flow velocities in which the transfer of the active ion to the electrode surface is as slow as that the mass transfer controls the rate of system.

Keywords Electrochemical mass transfer · Reduction of ferricyanide · Electrochemical limiting current · Electrode material · Rotating disc electrode

1 Introduction

The electrochemical limiting current diffusion technique (ELDCT) has been employed for the transport phenomena measurements between liquids and a surface for about half a century [1–3]. It can be applied to the measurements of convective mass/heat transfer coefficient [4–10], diffusion coefficient [11, 12], and some flow hydrodynamic characteristics including flow velocity, flow direction, turbulence fluctuations and wall shear stress in a wide range of systems with any geometry [13–17], and more recently for mixing time measurement in stirred vessel [18, 19]. There are also some publications on the effect of the experimental conditions on the limiting current measurements [20–22]. The most commonly employed electrolyte system for this technique is potassium ferri-ferrocyanide couple supported by an inert electrolyte. Since gold and platinum which are excellent electrodes are expensive, nickel has been widely used as electrode in this sort of investigations. No work was spotted about the alternative electrode materials for the cathodic reduction of ferricyanide for transport phenomena studies.

The aim of this work is to investigate whether some different metal alloys can be employed as electrodes in ELDCT having potassium ferri-ferrocyanide couple supported with an inert electrolyte. For this purpose, we investigated the usability of metal alloys in 8 different compositions for ELDCT works by the rotating disc electrode (RDE) technique.

1.1 Electrochemical limiting diffusion current technique

In an electrochemical system in which the heterogeneous redox reactions take place on the electrodes, different mechanisms make contribution to the transfer of active ions between the electrode surface and bulk solution.

✉ Sinan Yapici, sinan.yapici@inonu.edu.tr | [1]Department of Chemical Engineering, Engineering Faculty, Inonu University, 44210 Malatya, Turkey.

These mechanisms are [23, 24]: 1- diffusion due to the concentration gradient of active ion between electrode surface and bulk solution, 2- migration of active ion due to electric potential gradient, and 3- transfer of the active ion by bulk motion of the electrolyte.

Therefore, when mass transfer is unidirectional (y), the net flux is the result of the total effect of these three contributions, and can be expressed by "Nernst-Planck equation":

$$J_A(y) = -D_A\frac{dC_A(y)}{dy} - \frac{nF}{\overline{RT}}D_AC_A(y)\frac{\partial\phi(y)}{\partial y} + v_A(y)C_A(y) \quad (1)$$

where J_A is molar flux of active ion (mol/m^{2}s); D_A, diffusion coefficient of active ion in electrolyte (m^2/s); F, Faraday constant (96 485 C/mol); $\overline{R}$, the universal gas constant (J/mol K); T, the absolute temperature (K); C_A, the concentration of active species (mol/m^3); υ_A, the velocity of active ion (m/s); ϕ, electric potential (V), and y, mass transfer direction (m). The total current density arising from these three contributions can be expressed as:

$$i = i_D + i_M + i_C = nF\left(J_{D,A} + J_{M,A} + J_{C,A}\right) = nF\left(-D_A\frac{dC_A(y)}{dy} - \frac{nF}{\overline{RT}}D_AC_A(y)\frac{\partial\phi(y)}{\partial y} + v_A(y)C_A(y)\right) \quad (2)$$

where i_D, i_M and i_C are the contributions of the diffusion which is originated from concentration difference, the migration due to polarisation in the system, and the bulk movement in mass transfer region, respectively, to the electric current.

Figure 1 shows the concentration and electric potential gradients, and mass transfer contributions for the species reducing at cathode according to two approaches: boundary layer and stagnant film (Nernst diffusion layer). In an electrolyte system, in the region far away from the electrodes, the dominant mass transfer mode is convection. However, in the film layer next to the electrodes, which is the mass transfer region, the bulk velocity of the active species in the transfer direction is negligible. Migration has a contribution along the distance between cathode and anode if the conductivity is not high enough. If the solution contains electrolytes, either active ions or inert species, in higher concentrations, the conductivity of the electrolytic solution also becomes higher, and the electric potential gradient between the electrodes can be assumed to be negligible. In this case, Eqs. (1) and (2) reduce to the following expressions, respectively:

$$J_{D,A} = -D_A\frac{dC_A(y)}{dy} \quad (3)$$

$$i_D = -nFD_A\frac{dC_A(y)}{dy} \quad (4)$$

and the rate of the process becomes diffusion, or mass transfer controlled. In the electrolyte systems under these conditions, the current is called the limiting diffusion current [25, 26].

When the electrochemical system is under steady state condition, Eq. (3) can be combined with convective mass transfer expression in the form of Newton's cooling law and Faraday's second law [5]:

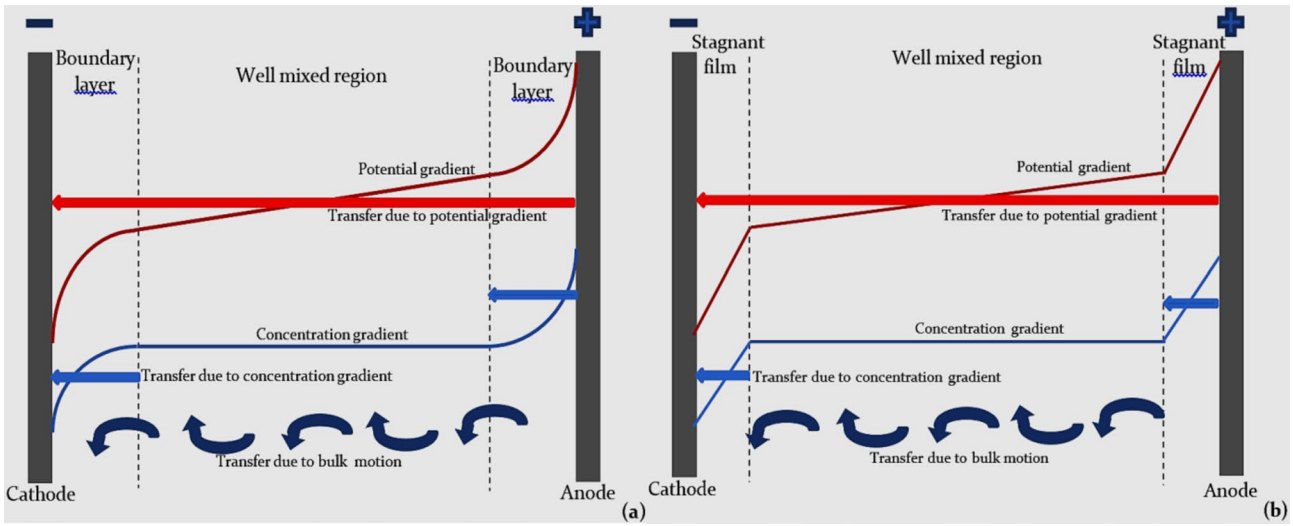


Fig. 1 Gradients and mass transfer contributions for the species reducing at cathode: **a** according to boundary layer approach, **b** according to stagnant film (Nernst diffusion layer) approach

$$J_{D,A} = -D_A \left.\frac{dC_A(y)}{dy}\right|_{y=0} = \frac{D_A}{\delta} C_A = k_c C_A = \frac{i_D}{AnF} \quad (5)$$

There are a number of electrolytic system which can be used for ELDCT measurements. The most popular ones are the reduction of potassium ferricyanide at platinum or nickel cathode and the reduction of copper in acidic copper sulphate solution at copper electrode [5]. For transport phenomena measurements the system having ferricyanide is preferred because of the following reasons [1, 2]: (1) It does not generate any precipitation on the electrode, therefore does not cause any deformation of the original surface. (2) With the addition of ferrocyanide, the original concentration can be maintained constant during the process since ferrocyanide oxidizes to ferricyanide at anode at the same stoichiometric ratio. (3) Cathodic reduction of ferricyanide provides a well-defined, wider and smoother plateau.

The redox reactions taking place in the system are:

$$\text{At cathode}: \left[Fe(CN)_6\right]^{3-} + e^- \rightarrow \left[Fe(CN)_6\right]^{4-} \quad (6)$$

$$\text{At anode}: \left[Fe(CN)_6\right]^{4-} \rightarrow \left[Fe(CN)_6\right]^{3-} + e^- \quad (7)$$

In a system having inert electrolytes, the current–potential (*IV*) behaviour is given in Fig. 2. There are three distinctive parts in this curve. In the first region in which the applied over voltage is lower, the rate of the electrochemical reaction is slower than that of mass transfer of active species to the surface. Therefore, the rate of the process is limited by reaction rate. However, increasing overvoltage enhances the reaction rate and after a certain value, it becomes faster than mass transfer rate. After this overvoltage value, the process rate is controlled by the mass transfer to the surface and current remains almost constant unless the hydrodynamic conditions are altered. This region in which the current does not change with increasing over voltage is called limiting diffusion current region. The corresponding current value is "limiting diffusion current". Since, under these conditions, the reaction rate is much faster than mass transfer rate, the active species are consumed as soon as they reach at electrode surface and practically the concentration of active species becomes zero at the surface. In the third region, a further increase in voltage causes the occurrence of side reaction(s) or the dissociation of the solvent, and therefore resulting in further increase in current. For the measurements in ELDCT, a voltage corresponding to around the centre of the plateau region is applied [20, 27, 28].

Although ELDCT has some difficulties similar to those encountered in other techniques depending upon which the physical or chemical changes upon which it based, it has also some important advantages of: (1) The properties of the system can be controlled easily. (2) The applied voltage and current can be monitored and controlled practically, (3) the experimental data which is current can be recorded, stored and processed easily. (4) It does not need a complicated, high-tech measurement system [29, 30].

In the application of ELDCT with ferri/ferrocyanide system the following precautions have to be observed:

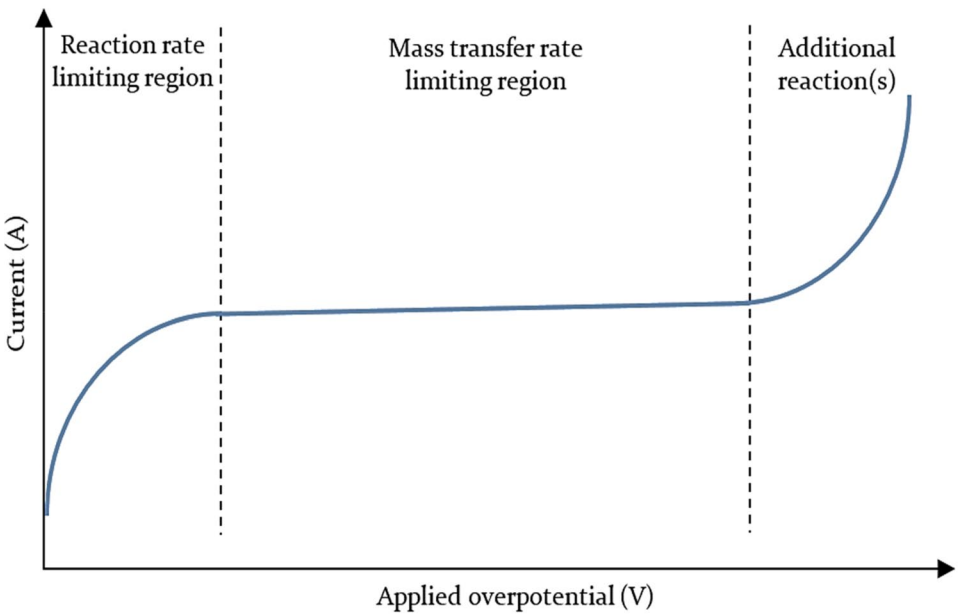


Fig. 2 *IV* behaviour for an electrochemical system exhibiting a good limiting-current plateau

1. Since the cathodic reduction of ferricyanide gives wider and smoother limiting diffusion plateau, to guarantee a cathodic controlled process, the concentration of ferrocyanide must be higher than that of the ferricyanide, and the surface area of anode electrode also must be larger than that of the cathode electrode.
2. The temperature control is of vital importance since the thermo-physical properties affecting mass transfer, such as diffusion coefficient, viscosity, reaction rate constant are temperature dependent.
3. The critical electrolyte flow rate which limits a mass transfer controlled process must be observed.
4. The concentration of the inert electrolyte which is added to avoid the migration by increasing the conductivity of electrolytic solution should be kept in an optimum level. It should be as high as to make the migration negligible, but also not to be too high to avoid the use of diffusion theories and transport coefficients. A range between 0.5 and 1 N is advised. Inert electrolytes, which are too corrosive, should be avoided.
5. The system and electrolyte should not be subjected to light since ferri- and ferrocyanide dissociate to hydrogen cyanide and hydroxide.
6. The oxygen dissolved in water should be stripped by an inert gas before the preparation of the electrolyte, and the solution should be kept under an inert gas blanket to avoid the negative effect of oxygen such as generating oxide layer on the electrodes or the oxidation of ferrocyanide during the process.
7. The electrodes should be prepared with care before the experiments. They must be first mechanically cleaned and finely polished, then be cleaned off from greases with an organic solvent, washed with distilled water, and be activated electrochemically by applying an overvoltage to evolve hydrogen gas on the cathode [20].

In the studies related to ELDCT, rotating disc electrode is frequently employed because of its easily measurable surface area, well defined hydrodynamic conditions and completely solved velocity profile.

1.2 Rotating disc electrode

The measurement techniques in the electrochemistry involving convective mass transfer of active ions can be called hydrodynamic methods. These techniques have the advantages of reaching at steady state more quickly and giving a facility of more precise measurements. The rotating disc electrode (RDE) is a convective system for which the rigorous solutions of hydrodynamic and mass transfer equations were carried out for steady-state conditions. RDE comprises of a cylindrical electrode sealed in a nonconductive insulator such as glass, Teflon, epoxy or any other plastic with one cylindrical end is open to function as electrode, as shown in Fig. 3.

The cell is designed and constructed in a way that the cell walls and other auxiliaries have no hydrodynamic effects on the convective transport between disc surface and bulk electrolyte, no edge effects of the disc electrode on the transport process [23, 30].

Since RDE is employed in laminar flow conditions, it is applicable in a certain range of rotational speed (ω). The lower limit for ω is the speed that hydrodynamic boundary layer thickness approaches to the disc radius. From the equation of hydrodynamic boundary layer thickness, the lower limit of rotation rate is:

$$\omega > 13\frac{\nu}{r_1^2} \tag{8}$$

where ν is the kinematic viscosity of the electrolytic solution (m^2/s). The upper limit is the flow conditions in which turbulent flow prevails. The critical Reynolds number for the transition from laminar to turbulent for RDE is $Re_{cr} = 2 \times 10^5$. Therefore, from $Re = \omega r_1^2/\nu$ for RDE, the upper limit of rotation speed can be deducted as:

$$\omega < 2 \times 10^5 \frac{\nu}{r_1^2} \tag{9}$$

To attain a steady concentration gradient, voltage-current scanning rate should be smaller enough compared to

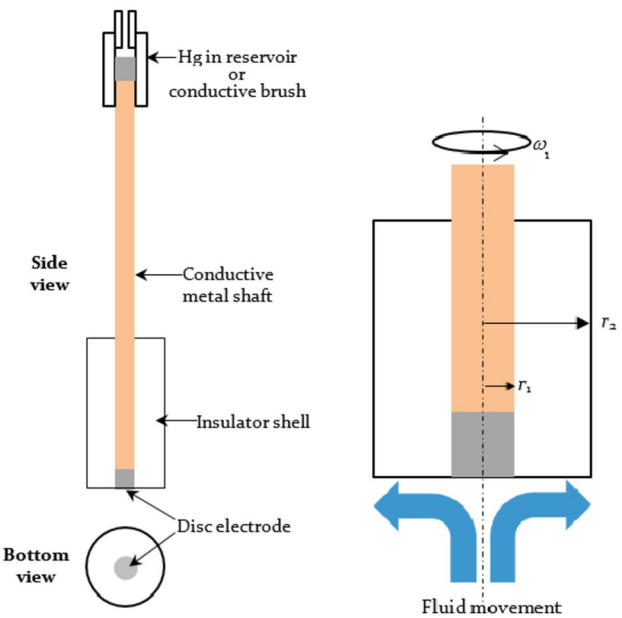


Fig. 3 Schematic illustration of rotating disc electrode

the rotation speed. The applied scanning rate is between 1 and10 mV/s with linear scanning voltammogram [25, 30].

2 Materials and method

In the experiments, metallic alloys with 8 different compositions were chosen as electrodes according to their constituent metals and the ratios of these metals. The electrodes were provided from Askaynak Inc., and their compositions are given in Table 1. The alloys in cylindrical rod with a radius of 3.25 mm and a length of 140 mm were designed and machined as rotating disc electrodes (working electrode; cathode). Epoxy resin was employed as isolation shell. After covering the electrode with the shell by using a mould, in such a way that the centre of the alloy rod will be orientated concentrically at the centre, and then the end disc surface was machined carefully and polished finely to get a smooth circular surface. The remaining part of the rod was electrically isolated (see Fig. 4.)

The same material as the cathode was employed as counter electrode (anode), which was made of a rod with the diameter of 3.25 mm the length of 140 mm and rounded spirally with a diameter of larger than that of the cylindrical insulator shell of disc electrode. It provided an anodic area of approximately 500 times larger than that of the cathode. This electrode was so placed concentrically around the working electrode that it does not affect the rotation of the disc .

For the electrochemical systems with no major fluctuations in ionic activity, a noble metal (e.g. a platinum or gold wire) can be employed as reference electrode [31]. Since the concentration of the active species in the present work remains constant during the experiments due to the characteristics of the chosen electrolyte system of the ferri/ferro cyanide, a bare part of 1 cm of an isolated thin platinum wire with a diameter of 0.1 mm was used as reference electrode.

The experiments were performed in a jacketed glass vessel of 1 L. The temperature of the reaction medium was kept constant at 25 ± 0.5 °C by using a circulator thermostat (Labo P300-D22). A digital controlled stirrer (IKA RW20) supplied the rotation of RDE. The electrolytic solution was an aqueous solution containing $K_3[Fe(CN)_6]$,

Table 1 Composition of the electrode materials

Convt. code	Composition (% in w)										Group
	C	Si	Mn	Cr	Ni	Fe	Cu	Mo	Other		
SD-HSS	0.90	1.20	1.30	4.50	–	81.30	–	7.50	W: 1.8	V: 1.5	1st
P-308-L	0.03	0.80	0.70	19.00	10.00	69.47	–	–	–		
P-308-Mn	0.10	0.50	6.00	18.00	9.00	66.40	–	–	–		2nd
P-308-Mo	0.05	0.35	2.50	19.00	10.00	65.60	–	2.50	–		
P-310-R	0.10	0.60	1.70	26.00	21.00	50.60	–	-	–		
Pik-55	1.00	–	–	–	56.00	43.00	–	–	–		3rd
Pik-65	0.50	0.40	1.00	–	65.10	3.00	30.00	–	–		
Pik-98	1.00	–	–	–	99.00	–	–	–	–		



Fig. 4 Photos of working electrodes designed as RDE

$K_4[Fe(CN)_6]$, and K_2CO_3 which is inert electrolyte. The concentration of ferrocyanide was maintained four times higher than that of ferricyanide. The solution was prepared by using high-grade chemicals, and micro filtrated ultra-pure water. For the determination of the limiting current, the electrochemical measurements, that are the potential between the working and reference electrodes versus current readings, were carried out at a scanning rate of 5 mV/s by chronoamperometry technique with the device of Gamry Potentiostat/Galvanostat (Interface 5000E ZRA). The experimental system is shown schematically in Fig. 5. After taking the necessary precautions for ELDCT application, the measurements were taken by applying over-potential from – 1.5 to 0.00 V at the rotational rates of 200 rpm, 1000 rpm and 2000 rpm. The readings were exhibited as current–voltage (*IV*) plots.

3 Results and discussion

According to composition of metallic alloys and the similarities in the behaviour of *IV* curves, the metallic alloy electrodes were evaluated in three different groups: SD-HSS and P-308-L in the first group, P-308-Mn, P-308-Mo and P-310-R in the second one, and Pik-55, Pik-65 and Pik-98 in the third.

For the first group alloy, their current–potential curves exhibited similar behaviour, as shown in Figs. 6 and 7 for SD-HSS and P-308-L coded electrodes, respectively. The limiting current plateaus are not smooth, and the current continues gradually to increase in the plateau region with the voltage. Even though this increase is partially reduced and a smoother and wider plateau region is attained with reduced rotational speed, the plateau is not yet well defined and smooth and the limiting current conditions are not fully met.

The SD-HSS coded electrode comprises of mainly Fe and contains 7.5% Mo and 4.5% Cr and Mn, W and V between 1.2 and 1.6%. The IV curves show that these metals in this level of content do not make any observable positive contribution to the electrode activity of the alloy. For P-308-L, Cr content of the material is approximately 4 times higher, and 10% Ni is available in the alloy instead of Mo in SD-HSS. However, still the IV behaviour is similar to that of SD-HSS and no improvement is observed in the electrode character with the partial change of metal species and composition.

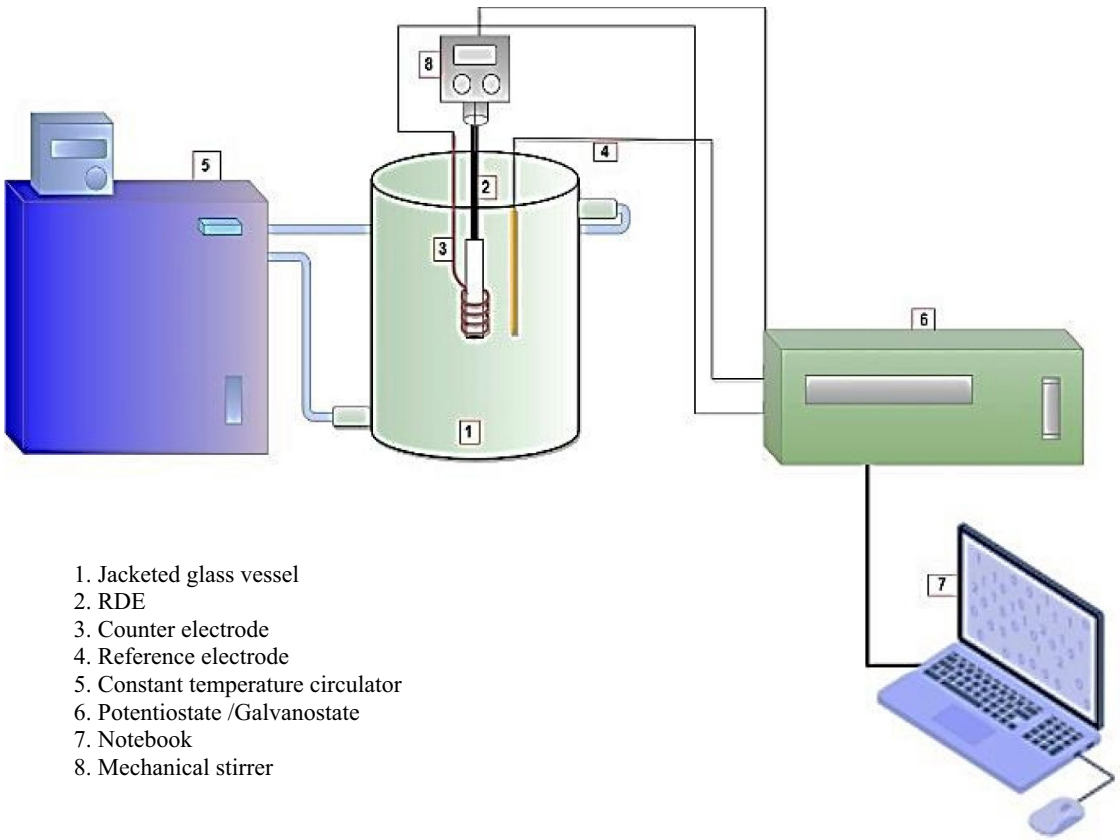


Fig. 5 Schematic view of experimental system

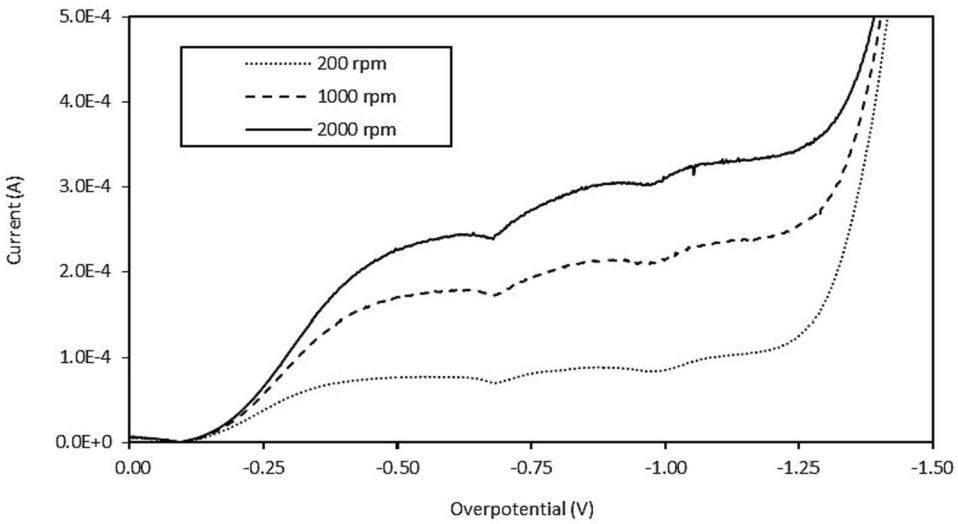


Fig. 6 *IV* curve for electrode of SD-HSS

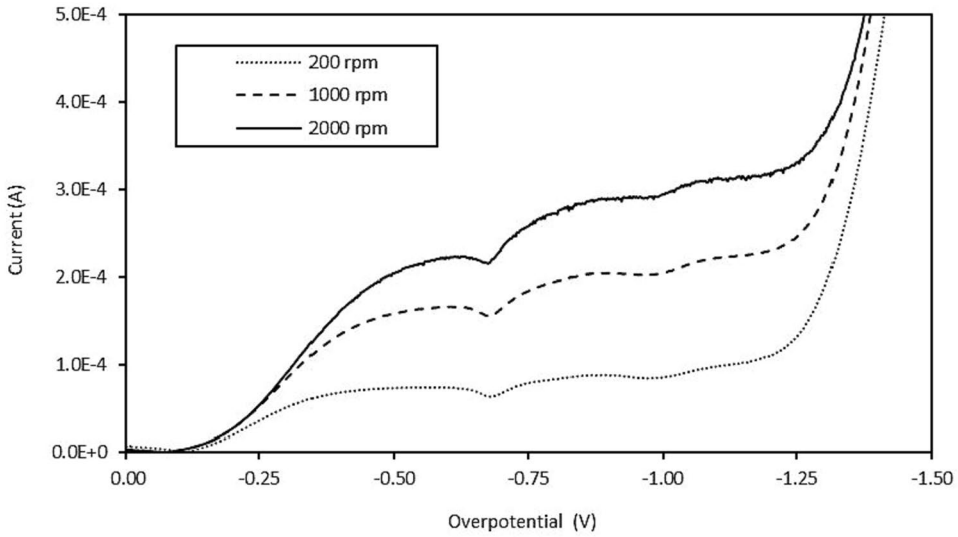


Fig. 7 *IV* curve for electrode of P-308-L

The limiting current appears at around – 0.35 V for the rotational speed of 200 rpm, shifts towards to approximately – 0.45 V with increasing rotational rate for this group of electrode. The generation of hydrogen at the cathode with the dissociation of water which determines the end of the plateau region starts at a voltage between – 1.17 and – 1.26 V, showing a tendency of increasing with rotational speed. As the rotational speed decreases, the plateau region becomes wider and smoother. The width of plateau region is around 0.85 V as potential difference for 200 rpm, and reduces to 0.75 V with increasing rotational speed for both electrodes. The deviations of the current value at the beginning and at the end of the plateau from the one read at centre voltage value are between approximately 10–30%.

For the second group of electrodes, IV curves are given in Figs. 8, 9 and 10. The limiting current starts around -0.50 V at 200 rpm and shifts towards -0.80 V with increasing rotation. The dissociation of solvent starts to occur at a voltage between – 1.28 and – 1.31 V for the electrodes of P-308-Mn and P-308-Mo, between – 1.25 and – 1.28 V for P-310-R, showing a tendency of increasing with rotational speed. Here, the width of the plateau is narrower than the first group, but smoother. The width of the plateau region increases with decreasing rotational speed from approximately 0.45 to 0.76 V as potential difference. It is narrower than the first group, but smoother. The current readings at the beginning and at the end of the plateau regions from those read at the centre voltage value show a deviation between about 7–32%, which is quite close to those in the first group electrodes. The change in Mn content between 1.70 and 6.00%, and different Cr and Ni content between 18 and 26% and 9 and 21%, respectively, do not

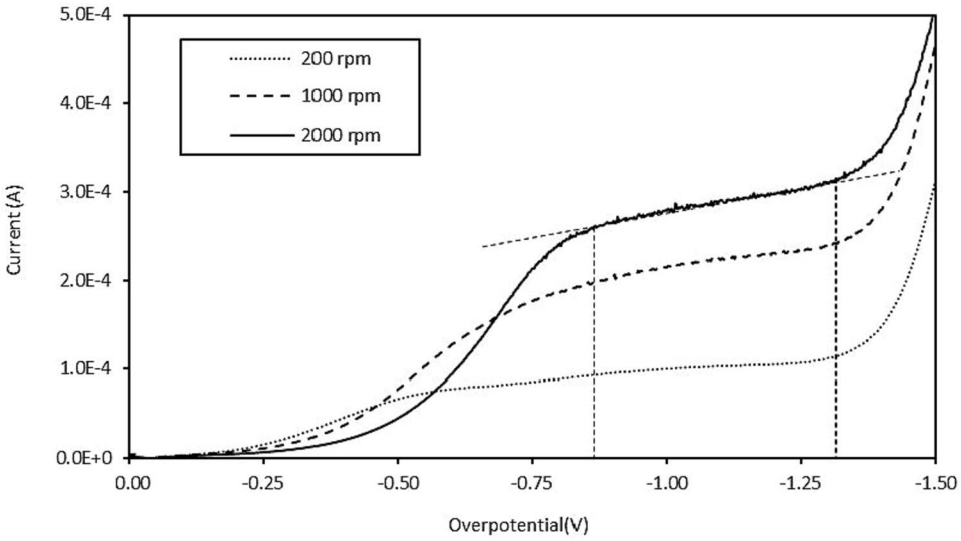


Fig. 8 *IV* curve for electrode of P-308-Mn, and determination of plateau region

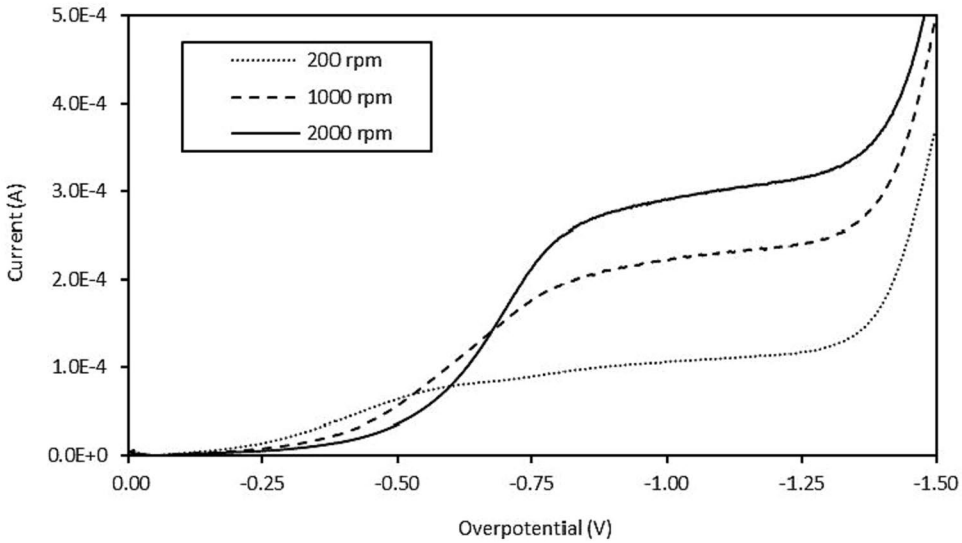


Fig. 9 *IV* curve for electrode of P-308-Mo

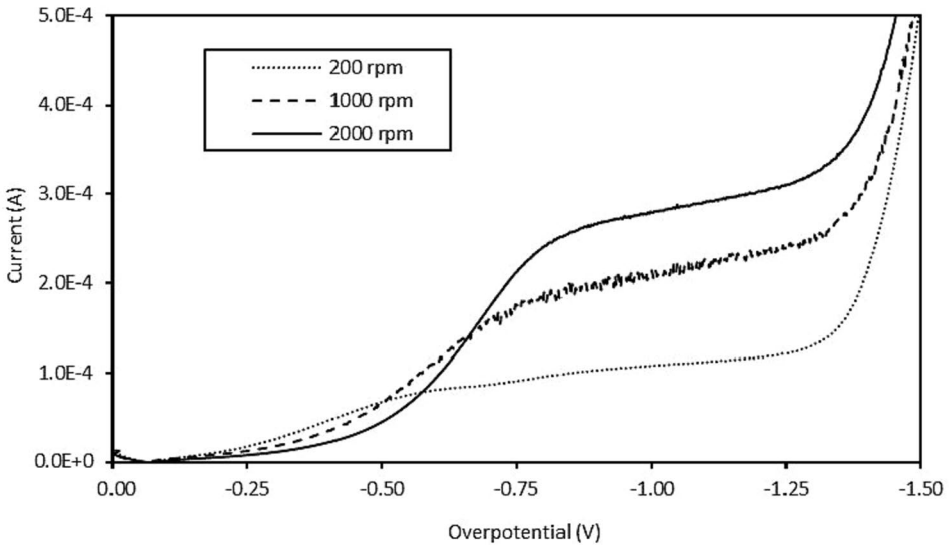


Fig. 10 *IV* curve for electrode of P-310-R

make any serious positive contribution to the improvement of ELDCT plateau region.

For the third group of electrodes, which stand out with their Ni contents, the IV curves are exhibited in Figs. 11, 12 and 13. Pik-55 alloy, consisted of mainly 56% Ni and 43% Fe, gives fairly smooth plateau regions. Increasing Ni content causes the limiting current to start much earlier, approximately between – 0.30 V and –0.55, with a tendency of increasing with rotation speed. The width of plateau region changes between 0.70–0.90 V as potential difference (Fig. 11). The high copper content in Pik-65 alloy increases the width of the plateau region, but does not result a pronounced improvement for the smoothness, even though its Ni content is approximately 10% higher (Fig. 12). The *IV* curves in the plateau region are still inclined except the *IV* curve for 200 rpm. The limiting currents are attained even much earlier at smaller overpotential differences at about – 0.1 V. The width of the plateau regions for this electrode is almost the same and approximately 1.17 V as potential difference. The dissociation of water starts at an overvoltage between – 1.24 and – 1.29 V.

Pik-98 consisted of almost pure Ni exhibited well defined, wide and especially smooth plateau regions for all rotational speeds, as seen in Fig. 13. The smoothness of the plateau region still exhibits improvement with decreasing rotational speed. The limiting current starts to occur at small overpotential differences at around – 0.1 V. The width of the plateau is between approximately 0.9–1.10 V. This electrode does not give the widest but smoothest plateau regions. For the third group of electrodes, the deviation in the current

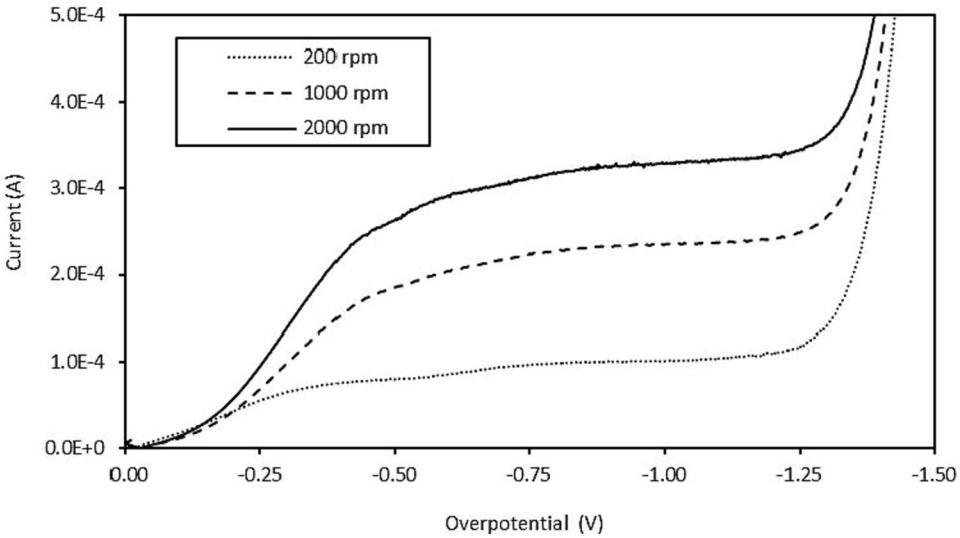


Fig. 11 *IV* curve for electrode of Pik-55

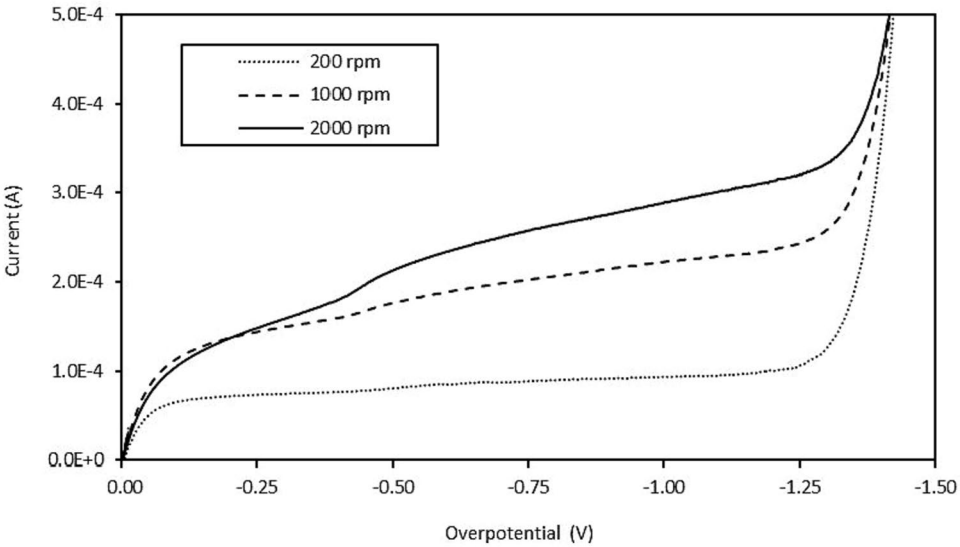


Fig. 12 *IV* curve for electrode of Pik-65

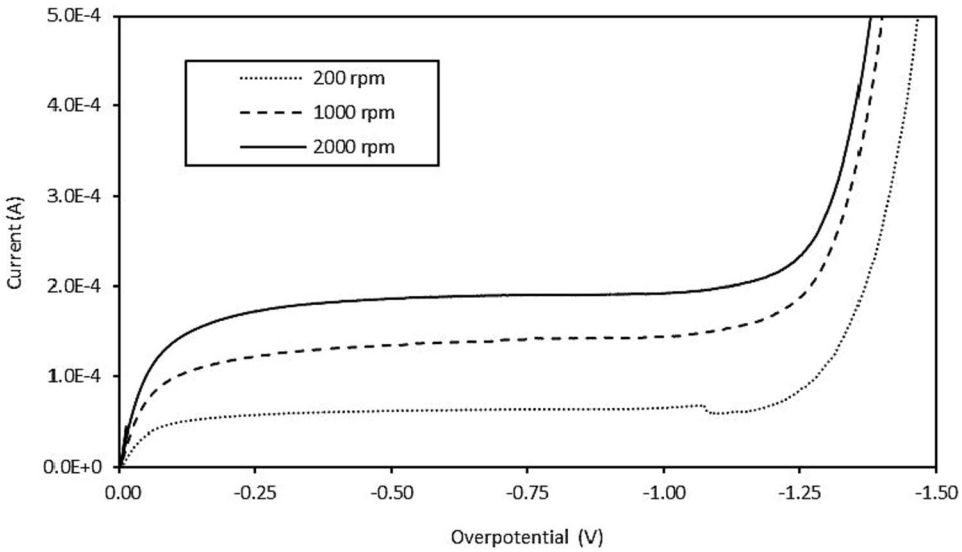


Fig. 13 *IV* curve for electrode of Pik-98

readings at the beginning and at the end of the plateau regions from those read at the centre voltage is between about 4–13%. The dissociation of solvent starts at much smaller potential differences of about – 1.10 V. The value of over potential depends on how it was measured: whether it was measured against a reference electrode or the counter electrode. However, for Ni electrode, the results of the present work are in compliance with the measurements in the literature using the same system. The widths of the plateau in those studies fall in almost the range of this work [7, 21, 32]

In Figs. 6 and 7, the peak-like behaviour or instabilities in the plateau region on the curves of SD-HSS and P-308-L in the voltage regions of – 0.6 to – 0.75 V and – 0.9 to – 1.1 V can be resulted from the temporary passivation of the electrodes, since no other redox reaction is expected because the solution is stripped off dissolved oxygen before measurement and ferricyanide does not give any other redox reaction in the applied potential difference range. This behaviour which does not appear on the curves of other electrodes may be resulted from the electrode composition or some uncontrollable contamination.

The general tendency of the decrease in the plateau's width with rotational rate for all the electrodes can be explained by the thinning of the diffusion layer with increasing flow rate. Increasing the rotational speed causes the hydrodynamic boundary layer to decrease according to the following equation obtained from the solution of hydrodynamic equations at steady state for rotating disc [30]:

$$\delta_h = 3.6(v/w)^{1/2} \quad (10)$$

Since the relation between diffusion boundary layer and hydrodynamic boundary layer can be expressed by the relation of $\delta_c \approx \delta_h Sc^{1/3}$, the thickness of the diffusion boundary layer will also decrease with increasing rotational speed. In this case, the concentration gradient across diffusion boundary layer in Eq. (4) becomes sharper and the transfer of active ion becomes faster. The reaction rate continues to become rate limiting step for a while until the applied overvoltage provides the driving force in order that the redox reaction becomes faster than the diffusion rate. Thus, the limiting current is reached at higher overvoltage, resulting in narrower plateau region. The inclined curves at plateau regions at high rotational speeds stem from the fact that the concentration of active ion does not reduce to zero since the electrochemical activity of the electrode is not enough to provide the redox reaction at higher rates compared to that of mass transfer. Therefore, for the rotational speed of 200 rpm in which the mass transfer rate is lower, all the electrodes gave reasonably well defined and smooth plateau region. The dissociation of water started at about – 1.10 V for Pik-98, while for the other electrodes it began at an overvoltage difference between approximately – 1.20 and – 1.30. This also shows the electrochemical activity of Pik-98 is higher than that of the other electrodes. Under the light of these findings, it can be concluded that only the electrode consisted of almost pure Ni can be safely used for ELDCT measurements. Other alloys may have a potential use in very low rotational speeds.

4 Conclusions

In this study in which 8 alloys with different metal composition were tested as electrode for the cathodic reduction of ferricyanide, the limiting current plateau was observed for all the electrodes, but a long, well defined and smooth plateau could not be obtained for all. As a result, it was determined that the presence of other metals, except the ones with Ni with a content higher than 50%, did not have a positive effect on the electrode activity and did not fully provide the limiting diffusion current conditions.

Electrodes with higher nickel content gave better, well-defined plateau regions. It has been determined that electrodes with different metal composition are not suitable at high flow rates and cannot be an alternative as working electrode to those of nickel and gold in ELDCT, and might be used at low flow rates as electrode in low flow velocities in which the transfer of the active ion to the electrode surface is as slow as that the mass transfer controls the rate of system.

Funding The financial support of Inonu University under project of BAP-FYL-2019-1651 is greatly appreciated.

Declarations

Conflict of interest The authors declare that there is no financial/personal interest that could affect our objectivity, and that no potential conflict exists.

Animal and human rights This work does not contain any study with human participant**.**

Open Access This article is licensed under a Creative Commons Attribution 4.0 International License, which permits use, sharing, adaptation, distribution and reproduction in any medium or format, as long as you give appropriate credit to the original author(s) and the source, provide a link to the Creative Commons licence, and indicate if changes were made. The images or other third party material in this article are included in the article's Creative Commons licence, unless indicated otherwise in a credit line to the material. If material is not included in the article's Creative Commons licence and your intended use is not permitted by statutory regulation or exceeds the permitted use, you will need to obtain permission directly from the copyright holder. To view a copy of this licence, visit http://creativecommons.org/licenses/by/4.0/.

References

1. Newman J (1968) Engineering design of electrochemical systems. Ind Eng Chem 60:12–27
2. Mizushina T (1971) The electrochemical method in transport phenomena. Adv Heat Transfer 7:87–161
3. Wragg A (1977) Applications of the limiting-diffusion-current technique in chemical engineering. Chem Eng 316:39–44
4. Selman JR, Tobias CW (1978) Mass-transfer measurements by the limiting-current technique. Adv Chem Eng 10:211–318
5. Landau U (1981) Determination of laminar and Turbulent mass transport rates in flow cells by the limiting current technique, Tutorial Lectures in Electrochemical Engineering and Technology, Edts: Alkire R, Beck T, AIChE Sym S, 77(204):75–87
6. Selman JR (1981) Techniques of mass transfer measurement in electrochemical reactors, Tutorial Lectures in Electrochemical Engineering and Technology, Edts: Alkire R, Beck T, AIChE Sym S 77(204): 88–102
7. Scottá K, Lobato J (2002) Determination of a mass-transfer coefficient using the limiting-current technique. Chem Educator 7:214–219
8. Barlak S, Yapıcı S, Sara ON (2011) Experimental investigation of pressure drop and friction factor for water flow in microtubes. Int J Therm Sci 50:361–368
9. Wilk J (2014) A review of measurements of the mass transfer in minichannels using the limiting current technique. Exp Therm Fluid Sci 57:242–249
10. Soliman MS, Nosier SA, Hussein M, Sedahmed GH, Mubarak AA (2017) Mass and heat transfer behavior of a new heterogeneous stirred tank reactor with serpentine tube baffles. Chem Eng Res Des 124:211–221
11. Hıraoka S, Yamada I, Ikeno H, Asano H, Nomura S, Okada T, Nakamura H (1981) Measurement of diffusivities of ferricyanide and ferrocyanide ions in dilute solution with KOH supporting electrolyte. J Chem Eng Jpn 14:345–351
12. Eroğlu E, Yapıcı S, Şara ON (2011) Some transport properties of potassium ferri/ferro-cyanide solutions in a wide range of Schmidt numbers. J Chem Eng Data 56:3312–3317
13. Rode S, Midoux N, Storck A (1995) Gas-liquid flow mechanisms in trickle beds operating in dispersed bubble and pulse flow. Chem Eng Res Des 73(A3):275–279
14. Yapıcı S, Yazıcı G, Özmetin C, Erşahan H, Çomaklı Ö (1997) Mass transfer to local electrodes at wall and wall friction in decaying turbulent swirl flow. Int J Heat Mass Tran 40:2775–2783
15. Sobolik V, Wein O (2008) The Levich problem with an eccentric segmented electrode on rotating disk. Russ J Electrochem 44(4):424–433
16. Bograchevz DA, Davydov AD (2008) The limiting current of electrochemical reaction in the binary electrolyte in the rotating electrochemical cell. Russ J Electrochem 44(10):1180–1184
17. Hanratty TJ (2014), Research of Thomas J. Hanratty 1951–2008, (Revised 2014), University of Illinois Urbana, 13–16
18. Aydin Ö, Yapici S (2018) A novel method for the measurement of mixing time: a new application of electrochemical limiting diffusion current technique. Exp Therm Fluid Sci 99:242–250
19. Aydın Ö, Arzutuğ MA, Yapıcı S (2019) A new application area of electrochemical limiting diffusion current technique: measurement of mixing time and effect of some parameters. SN Applied Sci 1(11):1364. https://doi.org/10.1007/s42452-019-1378-3
20. Berger FP, Ziai A (1983) Optimisation of experimental conditions for electrochemical mass transfer measurements. Chem Eng Res Des 61:377–382
21. Szanto DA, Cleghorn S, Ponce-de-Leon C, Walsh FC (2008) The limiting current for reduction of ferricyanide ion at nickel: the importance of experimental conditions. AIChE J 3:802–810
22. Zhong G, Xu S, Liu L, Zheng CZ, Dou J, Wang F, Fu X, Liao W, Wang H (2020) Effect of experimental operations on the limiting current density of oxygen reduction reaction evaluated by rotating-disk electrode. Chem Electro Chem 7:1107–1114
23. Nikolic J, Expósito E, Iniesta J, González-Garcia J, Montiel V (2000) Theoretical concepts and applications of a rotating disk electrode. J Chem Edu 9:1191–1194

24. Ciobanu M, Wilburn JP, Krim ML, Cliffel DE (2007) Fundamentals. Handbook of electrochemistry. Elsevier, pp 3–29. https://doi.org/10.1016/B978-044451958-0.50002-1
25. Cai W, Zhao X, Liu C, Xing W, Zhang J (2013) Electrode kinetics of electron-transfer reaction and reactant transport in electrolyte solution in rotating electrode methods and oxygen reduction electrocatalysts. In: Xing W, Yin G, Zhang J (eds.), Elsevier, Amsterdam, pp 33–65
26. De França Neta LS, Borges CP, Habert AC (2017) Evaluation of mass transfer in a novel hollow fiber module design using an electrochemical technique. Braz J Chem Eng 3:789–798
27. Scott K, Lobato J (2002) Determination of a mass-transfer coefficient using the limiting-current technique. Chem Educat 7:214–219
28. Fischl DS (1998) Effects of small flow obstacles on the limiting current and pressure drop in a square duct. M.S. Thesis, University of California, California
29. Cañizares P, García-Gómez J, Fernández de Marcos I, Rodrigo MA, Lobato J (2006) Measurement of mass-transfer coefficients by an electrochemical technique. J Chem Educ 8(83):1204–1207
30. Bard AJ, Faulkner LR (2001) Methods involving forced convection-hydrodynamic methods. Electrochemical methods: fundamentals and applications. Wiley, pp 280–3157
31. Zoski CG (2007) Handbook of electrochemistry. Elsevier, Amsterdam
32. Wilk J, Grosicki S (2018) Experimental study of electrochemical mass transfer in an annular duct with the electrolyte nanofluid. Int J Therm Sci 129:280–289

Publisher's Note Springer Nature remains neutral with regard to jurisdictional claims in published maps and institutional affiliations.